Development 134, 3941-3952 (2007) doi:10.1242/dev.007930

Broad, ectopic expression of the sperm protein PLCZ1 induces parthenogenesis and ovarian tumours in mice

Naoko Yoshida[1,*], Manami Amanai[1,*], Tomoyuki Fukui[1], Eriko Kajikawa[1], Manjula Brahmajosyula[1], Akiko Iwahori[1], Yoshikazu Nakano[1], Shisako Shoji[1], Joachim Diebold[2], Harald Hessel[3], Ralf Huss[3] and Anthony C. F. Perry[1,†]

Mammalian metaphase II (mII) exit and embryogenesis are induced at fertilisation by a signal thought to come from the sperm protein, phospholipase C-zeta (PLCZ1). Meiotic progression can also be triggered without sperm, as in parthenogenesis, although the classic mouse in vivo parthenogenetic model, LT/Sv, fails in meiosis I owing to an unknown molecular etiology. Here, we dissect PLCZ1 specificity and function in vivo and address its ability to interfere with maternal meiotic exit. Wild-type mouse *Plcz1* expression was restricted to post-pubertal testes and the brains of both sexes, with region-specifying elements mapping to a 4.1 kb *Plcz1* promoter fragment. When broad ectopic PLCZ1 expression was forced in independent transgenic lines, they initially appeared healthy. Their oocytes underwent unperturbed meiotic maturation to mII but subsequently exhibited autonomous intracellular free calcium oscillations, second polar body extrusion, pronucleus formation and parthenogenetic development. Transfer of transgenic cumulus cell nuclei into wild-type oocytes induced activation and development, demonstrating a direct effect of PLCZ1 analogous to fertilisation. Whereas *Plcz1* transgenic males remained largely asymptomatic, females developed abdominal swellings caused by benign ovarian teratomas that were under-represented for paternally- and placentally-expressed transcripts. *Plcz1* was not overexpressed in the ovaries of LT/Sv or in human germline ovarian tumours. The narrow spectrum of PLCZ1 activity indicates that it is modulated by tissue-restricted accessory factors. This work characterises a novel model in which parthenogenesis and tumourigenesis follow full meiotic maturation and are linked to fertilisation by PLCZ1.

KEY WORDS: Phospholipase C-zeta (PLCZ1), Oocyte activation, Fertilisation, Tumour, Embryo, Transgene

INTRODUCTION

Mammalian oocytes are typically arrested at meiotic metaphase II (mII) until a fertilising sperm induces cell cycle resumption and the initiation of embryogenesis. Multiple candidates for the causative sperm entity have been proposed (reviewed by Runft et al., 2002) and database searching presumptive of the involvement of phospholipase C (PLC) identified an erstwhile uncharacterised mammalian isoform, PLC-zeta (PLCZ1) (Saunders et al., 2002). PLCZ1 expression was reportedly restricted to the testis (Saunders et al., 2002) and shown by protein correlation profiling to be present in demembranated sperm (Fujimoto et al., 2004). PLCZ1 is unusual among PLCs because it lacks pleckstrin homology (PH) and Src homology (SH) domains; proceeding from the N- to the C-terminus, it comprises four EF hand domains, X and Y domains and a C-terminal C2 region (Saunders et al., 2002). PLCZ1 deletion analyses suggest that EF hand domains 1 and 2 (EF1 and EF2) are primarily responsible for phosphatidylinositol 4,5-bisphosphate (PIP_2) hydrolysis, whereas EF3 mediates its exquisite Ca^{2+} sensitivity (Kouchi et al., 2005). PIP, but not PIP_2, binding is mediated in vitro by the C2 domain, which may coordinate with Ca^{2+} sensing to regulate pulsatile Ca^{2+} release from oocyte stores (Kouchi et al., 2005).

Oscillations in the concentration of intracellular free Ca^{2+}, referred to as $[Ca^{2+}]_i$, initiate 1-3 minutes after mouse gamete membrane fusion (Jones et al., 1995; Lawrence et al., 1997) and are thought to modulate the activity of calmodulin kinase II (CAMK2) towards the cytostatic factor FBXO43 (also known as EMI2), potentiating secondary FBXO43 phosphorylation by PLK1 and targeting it for proteolytic degradation to induce meiotic exit (Lorca et al., 1993; Rauh et al., 2005; Shoji et al., 2006).

This model of PLCZ1 activity leaves several issues open. The PH domains of other PLC family members mediate their interactions with phosphoinositides, but PLCZ1 does not possess a PH domain and the PLCZ1 C2 domain does not bind to PIP_2 in vitro (Kouchi et al., 2005). PLCZ1 phospholipid targeting remains poorly understood and a simple interaction might not account for the generation of IP_3 – a prelude to Ca^{2+} release. Moreover, although ~1.25-2.5 fg of native PLCZ1 (corresponding to ~3-6% of the amount in a single sperm) efficiently induces oocyte activation, a ~120-240-fold excess of baculovirus-expressed PLCZ1 (300 fg) is required to induce $[Ca^{2+}]_i$ oscillations resembling those of fertilisation (Fujimoto et al., 2004; Kouchi et al., 2004). Premature attenuation or hyperstimulation of $[Ca^{2+}]_i$ oscillations does not prevent development to term (Ozil et al., 2006), showing that embryogenesis in the mouse is tolerant of a range of $[Ca^{2+}]_i$ dynamics during oocyte activation. Finally, distinct sperm-borne entities reduce the PLCZ1 signalling threshold (Perry et al., 1999b; Perry et al., 2000; Fujimoto et al., 2004) and play unresolved roles in meiotic exit (Manandhar and Toshimori, 2003; Sutovsky et al., 2003; Wu et al., 2007). These findings raise the possibility that multiple factors play a role in sperm-dependent meiotic resumption.

Sperm-independent meiotic resumption (parthenogenetic activation) can be induced by exposing mature mII oocytes to one of a multiplicity of exogenous non-physiological challenges in vitro,

[1]Laboratory of Mammalian Molecular Embryology, RIKEN Center for Developmental Biology, 2-2-3 Minatojima Minamimachi, Chuo-ku, Kobe 650-0047, Japan. [2]Institute of Pathology, University of Munich, Thalkirchner Str. 36, 80337 Munich, Germany. [3]Roche Diagnostics GmbH, Nonnenwald 2, D-82372 Penzberg, Germany.

*These authors contributed equally to this work
†Author for correspondence (e-mail: tony@cdb.riken.jp)

Accepted 8 August 2007

including electrical stimulation (Tarkowski et al., 1970), ethanol (Cuthbertson, 1983) and strontium chloride (Whittingham and Siracusa, 1978). In vivo, the two best-known models of sperm-independent meiotic interference are LT/Sv (Stevens and Varnum, 1974) and gene-targeted *Mos*-null mouse strains (Colledge et al., 1994). Independently targeted MOS-deficient oocytes exhibit aberrant spindle migration to produce an abnormally large and persistent first polar body (Pb_1) (Choi et al., 1996), deregulation of MAPK activity during oocyte maturation (Araki et al., 1996) and pronucleus formation following Pb_1 extrusion (Colledge et al., 1994); all reflect dysfunctional meiosis I, in contrast to parthenogenetic activation in vitro, which acts upon mature mII oocytes. Mice lacking MOS develop ovarian teratomas, which are accordingly likely to be a consequence of first meiotic deregulation. Teratomas occur in ~30% of MOS-deficient females when they are 4-8 months old, but not outside this age range; occasionally, the tumours are malignant and metastatic (Furuta et al., 1995).

Teratomas also occur in the other well-known model of maternal meiotic dysfunction, LT/Sv, although their incidence is slightly higher (37-52%) in females of 3-4 months, with tumours appearing as early as 2 months (Stevens and Varnum, 1974). LT/Sv oocytes frequently undergo mI arrest and/or fail to establish mII arrest (Hampl and Eppig, 1995), and it has been concluded that parthenogenetic activation potentiates teratoma formation (Stevens and Varnum, 1974). However, experiments aimed at rederiving LT/Sv from its progenitor strains (BALB and C58) revealed that mI arrest is necessary but not sufficient to elicit parthenogenetic activation (Eppig et al., 1996). Furthermore, some LT/Sv-related strains undergo mI arrest and parthenogenesis without developing teratomas (Eppig et al., 1996), showing that meiotic failure does not necessarily result in tumour formation. LT/Sv thus possesses a complex and polygenic phenotype and predisposing loci have been mapped to chromosomes 1, 6 and 9 (Lee et al., 1997; Everett et al., 2004). The single mouse *Plcz* gene, *Plcz1*, lies on chromosome 6.

We here evaluated PLCZ1 specificity by forcing its ectopic expression in a broad range of tissues, enabling us to determine whether this interfered with maternal meiosis. These experiments reveal that endogenous PLCZ1 induces activation of mature mII oocytes with a high degree of specificity in vivo, linking fertilisation to tumourigenesis and representing a unique model of parthenogenesis.

MATERIALS AND METHODS

Generation of *Plcz1* transgenic mouse lines

$B6D2F_1$ testis-derived *Plcz1* cDNA was amplified by PCR with primers (all are shown 5′ to 3′): GACAAGCGGCCCAGATCATG and GTCTAGATTACTCTCTGAAGTACCAAACATAAATAAAC. For the CS series (PLCZ1ctFLAG-i-Venus), a single FLAG epitope was introduced to generate a C-terminal fusion with PLCZ1 by PCR using ACATGCATGCACTAGTATGGAAAGCCAACTTCATGAGCTC and GGAATTCCATATGTCACTTGTCGTCATCGTCTTTGTAGTCCTCTC-TGAAGTACCAAACAT. An *Spe*I-*Nde*I PLCZ1-FLAG fragment downstream of the hybrid cytomegalovirus IE enhancer-chicken *Actb* promoter, *pCAG*, which is active in many tissues (Takada et al., 1997), and an *IRES-Venus* (*IRES*, internal ribosome entry site) cassette (our unpublished data), were introduced downstream of this. For the CV series (PLCZ1ctVenus), a *Plcz1* amplimer generated with the primers ACATGCATGCACTAGTATGGAAAGCCAACTTCATGAGCTC and GGAATTCCATATCCCCGGGCCCTCTCTGAAGTACCAAACATA was used to generate a fusion protein with the junction sequence YVWYFREARGSTMVS; the linker between the C-terminus of PLCZ1 (…FRE) and the start of Venus (MVS…) is underlined. For the generation of promoter-mapping constructs (see Fig. S1B in the supplementary material), a 4.5 kb *Plcz1* putative promoter fragment (*pPlcz1*) was amplified with TCAGAGGTCACCCAACACGG and TCCCCCGGGATTTCATGA-TCTGGGCCGC and used to generate *pPlcz1→Cre*. A 4.1 kb *Plcz1* fragment was removed from *pPlcz1→Cre* to produce *pPlcz1→Plcz1-FLAG* and *pPlcz1→Plcz1-FLAG-IRES-Venus*. All transgene (tg) constructs were introduced by mII transgenesis (Perry et al., 1999a) to produce founder (F_0) $B6C3F_2$ lines that were subsequently crossed with C57BL/6 unless stated otherwise. Mice were maintained according to local institutional guidelines.

Culture, manipulation and analysis of oocytes and embryos

Oocyte and embryo retrieval, manipulation and culture were essentially as described previously (Shoji et al., 2006; Yoshida and Perry, 2007). For movies, oocytes were transferred to a chamber (37°C, 5% CO_2) on the stage of a Zeiss Axiovert 200 microscope and collected as described (Shoji et al., 2006). Nuclear transfer was into $B6D2F_1$ mII oocytes essentially as described (Yoshida et al., 2007).

PCR

Analysis of mRNA was by PCR as described (Shoji et al., 2006; Amanai et al., 2006b). *Plcz1* transcripts in testis and brain samples (Fig. 1A) were amplified for 25 and 30 cycles, respectively. Amplification of *Cre* or recombinant *Plcz1* (*rPlcz1*) mRNAs in *pPlcz1* transgenic lines was with 30 or 35 cycles, respectively. RNA from clinical paraffin sections was isolated using a High Pure RNA Paraffin Kit (Roche) according to the manufacturer's instructions. First-strand cDNA was synthesized from 1 μg of isolated RNA using a Transcriptor First Strand cDNA Synthesis Kit (Roche) primed with 1 μl of 50 pmol/μl oligo$(dT)_{18}$ and 2 μl of 600 pmol/μl random hexamer in a final volume of 20 μl. One microlitre of each cDNA reaction was used per standard 25 μl PCR reaction. PCR reactions were typically accompanied by RT-minus (lacking reverse transcriptase) controls, performed on at least two independent preparations and where appropriate were examined following 2% (w/v) agarose gel electrophoresis. Ratiometric quantification of mRNAs (qPCR) was as described (Shoji et al., 2006; Amanai et al., 2006b). Amplification of *Venus* and *Plcz1* tgs (with *Plcz1* intron-flanking primers to avoid native gene amplification) in 8 ng of tumour or control genomic DNA was performed to estimate their relative genomic complements. The ratio of tg signal to endogenous control *Actb* or *H2afz* genomic DNA levels in (diploid) somatic tissue from hemizygotes was normalised to 1.0 and used as a calibrator for tumours. PCR primer sequences are given in Table 1.

Tissue sectioning

Following standard trans-cardial perfusion with PBS followed by buffered 4% (w/v) paraformaldehyde (PFA, Wako), ovaries for frozen sectioning were fixed in 4% PFA overnight at 4°C, and subsequently subjected to cryoprotection in 30% (w/v) sucrose (Wako) in PBS for 3 days. The samples were then embedded in OCT compound (Sakura, Tokyo) and sections (14 μm) prepared on a Microm HM560 cryostat (Microm, Walldorf). Sections were air-dried, washed in PBS and stained with Hoechst 33258 before being mounted in fluorescent mounting medium (DakoCytomation, CA) and analysed by confocal microscopy.

For histopathology, resected tumours were acutely fixed in 4% buffered PFA (pH 7.0) and embedded in paraffin by standard methods. Sections (1-2 μm) were deparaffinised, dried and stained with Haematoxylin and Eosin. Bright-field visualisation and image capture to enable classification (WHO) was on a Leica Microsystems Application Suite (Leica). Tumours were scored according to established parameters (World Health Organization, 2003).

Fluorimetric calcium imaging

Relative levels of ooplasmic $[Ca^{2+}]_i$ were determined for immature germinal vesicle (GV) and mI oocytes or mature mII oocytes. Immature oocytes were collected 48 hours after equine chorionic gonadotropin injection and analysed within 2 hours (GV oocytes) or 8-10 hours (mI oocytes) after collection. Mature, mII oocytes were analysed ~14.5 hours after human chorionic gonadotropin (hCG) injection. Prior to recording, oocytes were loaded for 30 minutes with 5 mM Fura 2 acetoxymethyl ester (Fura 2-AM; Molecular Probes) in a humidified atmosphere of 5% (v/v) CO_2 in air at

Table 1. PCR primer sequences

Gene	Forward (5′ to 3′)	Reverse (5′ to 3′)
RT-PCR primer sequences		
Actb	GGCATTGTTACCAACTGGGACGAC	CCAGAGGCATACAGGGACAGCACAG
Plcz1	TGACGACCATCCAGTTACCCTCAC	ACAACACGAGTCTGCTGCTTCACG
Venus	ACGTAAACGGCCACAAGTTC	GAACTCCAGCAGGACCATGT
Plac1	TCCACACGGAGAGAACAGAACTAAC	AGAAGGCGTCCAGGAAGGATTC
Gcm1	AAAGCCAGACAGAAGCAGCAGAGG	AAAAGATGAAGCGTCCGTCGTGCC
Zfp36l3	CAGTGATGACGAAGATGAAGACGAC	TGAGAAGCGGCTGAAGATGG
Plib (*Prl3d2*)	TTGGATAACAGACAGAACACTTCCC	CAGTCAGTGCAGACACCAGGTG
Tpbpa	CACAGCCAGTTGTTGATGACCC	TTTTTGCTTGCCCTTGCCCCAG
Ereg	TGGTCTGCGATGTGAGCACTTC	CCTTGTCCGTAACTTGATGGCAC
Ptgs2	CAACACACTCTATCACTGGCACCC	CATCTCTCTGCTCTGGTCAATGG
Mmp1a	CTTCAAAGGCAGGTTCTACATTCG	TCTTCCTCACAAACAGCAGCATC
Mmp2	CCTGGAATGCCATCCCTGATAAC	TAACTACAGAGGAGGACAGAGCCG
Eomes	ATCGTGGAAGTGACAGAGGACG	CGGGAAGAAGTTTTGAACGCC
Hand1	CAAGGCTGAACTCAAAAAGACGG	TCTCACTGGTTTAGCTCCAGCG
Psx1 (*Rhox6*)	TGAATAGGCTGGCTCAACTGCG	AAAGGGCTCTCCTCATCCGAAACC
Ets2	CAAGGCAAACCAGTTATTCCTGC	TTTTTCCTCTTCCCCCACCG
PLCZ1	CAAATGAAGCAGCAGACTCGTG	ACGTATCAATGCCAATTCTGGG
ACTB	TGACAGGATGCAGAAGGAGA	GCTGGAAGGTGGACAGTGAG
Cre	CATTTGGGCCAGCTAAACAT	CCCGGCAAAACAGGTAGTTA
qPCR (RT-PCR) primer sequences		
Actb	TGACAGGATGCAGAAGGAGA	GCTGGAAGGTGGACAGTGAG
Pou5f1	CGTGAAGTTGGAGAAGGTGGAACC	GCAGCTTGGCAAACTGTTCTAGCTC
Mos	CAGTGGTTGCCTACAATCTGCG	AGCCTTGAGGTCCCTTTGGAG
Nanog	GCAAGCGGTGGCAGAAAAAC	GCAATGGATGCTGGGATACTCC
Cdx2	GCAGTCCCTAGGAAGCCAAGTG	CTCTCGGAGAGCCCAAGTGTG
Sox2	GGAAAAAAACCACCAATCCCATCC	TTTGCGAACTCCCTGCGAAG
Fbxo43	AGTGGTGAGCAGGTTCCAACTCTG	TGTTTACTCCGTAGGTGGGTGAGG
Plcz1	TGACGACCATCCAGTTACCCTCAC	ACAACACGAGTCTGCTGCTTCACG
Igf2	CTAAGACTTGGATCCCAGAACC	GTTCTTCTCCTTGGGTTCTTTC
H19	TTGCACTAAGTCGATTGCACT	GGAACTGCTTCCAGACTAGGC
Mest	GGCTCCTCTATGATGGCCG	AAGCCTTTCTGAACAGCCAGC
Peg3	CAATCTATGAATGCCAGGACTGTG	CGACTGTCAACCAGAGCCTTTC
Nnat	CGAAAGCCCTCCCCAAAATG	TTGACCACAACTGCTGCGTGAGAC
Peg10	TGATGCCTCCAAACAGCCAGAC	CCTCCATTGCCACAGTAGAGACAC
Peg12	TTGCACATTTCCTGTGGGAC	GGGTCAGAAGGAGGAAATCAACTC
Peg13	ACTCAGAAGGGCATCTCACCTCTC	TTTGGCTTGGTTTGTTCACACC
Grb10	AATGGGTCCCCCAAGTTTTCT	CCGCAACCTGCAGAGAGC
Air	TGAGCAGGCACATTACCGAAGG	TTTTCCCCCACCCCTAAAGC
Cdkn1c	AGGAGCAGGACGAGAATCAAGAGC	GAAGAAGTCGTTCGCATTGGC
Impact	ACCGAAGGAGCACTTTTCAGGC	TAGGCATAGATGTTGTGGGTGGCG
Plagl1	GGACTTCCTGTGTCAGTTCTGTGC	TGCTCTGGTAATCTCCTGCCTG
Ascl2	TTCCAGTTGGTTAGGGGGCTAC	CTTGGCATTTGGTCAGGCTG
Pon2	AACCATCCTCCTGCATCAGAGGTC	GGACAGACCCGTTGTTGATATACAC
Copg2	GCAGAGACAGAGTATTTCGTTCGC	CACTTCATAGGAATCGGATGGTTC
Gtl2	TTGCACATTTCCTGTGGGAC	AAGCACCATGAGCCACTAGG
Zim1	CCAAAGAGAACGATGTTCCTGG	TGTCTTAGAATTGTCTGGCTTCCG
Htr2a	CTGAAAATCATTGCGGTGTGG	AAAGTTGTCATCGGCGAGCAGG
Dppa2	CGATGTCCTCTTCCGTCTAATGTG	AACCCAGGTCTGTCCAGCAAG
NM_026894	ATCTCATCAATCGTCAGACCTTCC	CCACCCTTTCCACATTTTGTTCAG
Rbp1	ATCCGCACGCTGAGCACTTTTC	CACTGGAGTTTGTCACCATCCC
Dab2	CTTCAAAGGCAATGCTCCTCC	TTATGGCTCCTGGGACCACAGTTG
Aurka	GCGGGAGAGACAAAGCAAGTTC	ATACAGCCTGAGGATGTTGGGGTG
Ptgs1	CGTTCACCCATTTCCTGCTGAC	GATAAGGTTGGACCGCACTGTG
Ptgs2	TCTCTACAACAACTCCATCCTCCTG	CACATTTCTTCCCCCAGCAAC
Elavl1	TTTCTCGGTTTGGGCGAATC	CCTGGGGGTTTATGACCATTG
Plk1	GTATTCCCAAGCACATCAACCCAG	GCCAGAAGTGAAGAACTCGTCATTG
Cd24a	TGCTCCTACCCACGCAGATTTAC	GTTACTTGGATTTGGGGAAGCAG
Kras	AACTGGGGAGGGCTTTCTTTG	ACCATAGGCACATCTTCAGAGTCC
Myc	TCCTTTGGGCGTTGGAAACC	TCGTCGCAGATGAAATAGGGC
Akt1	TTGTGTCTGCCCTGGACTACTTGC	CCGTTATCTTGATGTGCCCGTC
Trp53	TGGAAGACAGGCAGACTTTTCG	ATGATGGTAAGGATAGGTCGGCGG
Pcna	AAGAAGAGGAGGCGGTAACCATAG	GGAGACAGTGGAGTGGCTTTTG
Atm	CATAGACCTGGGAGTGGCTTTTG	TCCATCGTTTTTTCACAGCACC
Atr	CGAATGGGAAAAAGGTGGTCG	TGGTGCTAACCGATTTGTGTGC
Cdkn1a	GCAGACCAGCCTGACAGATTTC	TCCTGACCCACAGCAGAAGAGG

Table continued on following page.

Table 1. Continued

Gene	Forward (5′ to 3′)	Reverse (5′ to 3′)
qPCR (RT-PCR) primer sequences		
Chk1 (*Chek1*)	GCTTTCCTTGTGGGACACTGGTC	GCCAGGGGTTCTGTGAAGATCC
Brca1	TCAGGCTTGACCCCCAAAGAAG	TCACACACAAACTCCGCATCTG
Brca2	GACCACGAAGAAGACACAACACAG	CGCTGAAACAAGCCTCAAGGTG
Id2	AGCCTGCATCACCAGAGACCTG	TCATTCGACATAAGCTCAGAAGGG
Gcm1	AAAGCCAGACAGAAGCAGCAGAGG	AAAAGATGAAGCGTCCGTCGTGCC
Primer sequences for estimation of tg dosage		
Actb	TGACAGGATGCAGAAGGAGA	GCTGGAAGGTGGACAGTGAG
H2afz	GCGTATCACCCCTCGTCACTTG	TCTTCTGTTGTCCTTTCTTCCCG
Plcz1	TGACGACCATCCAGTTACCCTCAC	ACAACACGAGTCTGCTGCTTCACG
Venus	GCAGAAGAACGGCATCAAGGCC	TGCTCAGGTAGTGGTTGTCGGG
Primer sequences for promoter sequencing		
Plcz1	TCAGAGGTCACCCAACACGG	
	TTTTCCCTTGGTTCACGGC	
	TGGTAGCGGGGAACTTTAC	
	CCAAGACACCTCTCTAACATCC	
	TTACCCTTTTTGCTGTGTTGGTG	
	CCGTTCCAACACTCTCCATTGTC	
	GTATGCTGGTCTATGAAGAAGG	
	CCTGGGGGTAAACATTGTGATGAA	
		GATTTCATGATCTGGGCCGCT
		CAGACACAGAGAAAACATACCAC
		GCCATCAGCACTGCCAAAAATACTG
		GCAATGTGCTGAGAAAAACAG
		GGGGAAGAATAAGAAATCGTG
		TCCTTGGGCTACATAGTGC
		AGCACTCACCAGACCGAAG
		AGATGACAGTCCCTCTGCCG

37°C in KSOM. Oocytes were then placed on the 37°C-heated stage of an Eclipse TE2000-U inverted fluorescence microscope (Nikon). Fluorescence images were obtained at 10 second intervals following exposure at 340 and 380 nm (0.2 seconds apart), collected through a 490-530 nm emission filter and processed with AQUA COSMOS ratio imaging application software (Hamamatsu Photonics).

Antibodies and immunoblotting

Rabbit polyclonal antibodies against a C-terminal fragment of mouse PLCZ1 (PLCZ1ct, residues 111-648) were affinity-purified from immune serum using protein G-sepharose beads (Amersham).

For western blotting, tissues were extracted in HBS lysis buffer, containing 0.1% (w/v) sodium dodecyl sulphate (SDS), 0.5% (w/v) deoxycholate, 1.0% (v/v) Nonidet P40, 150 mM NaCl, 10% (w/v) glycerol and 50 mM HEPES (pH 8.0) and 20 μg protein analysed per sample. For immunoprecipitation, 1 mg/ml protein preparations were mixed with anti-FLAG-conjugated beads (Sigma) for CS, or anti-PLCZ1ct-conjugated protein G-sepharose beads (Amersham) for CV, at 4°C overnight. Beads were washed with HBS (CS) or a wash buffer containing 150 mM NaCl, 2 mM $CaCl_2$, 5 mM $MgCl_2$, 0.05% (v/v) Nonidet P40, protease inhibitor cocktail and 10 mM Tris-Cl, pH 7.5 (CV). Bound material was removed by boiling in sample buffer for 5 minutes. Immunoblotting was typically using enhancer with a LumiGLO Reserve Chemiluminescent Substrate Kit (Kirkegard and Perry Laboratories) as described previously (Shoji et al., 2006).

Epifluorescence microscopy

For immunofluorescence imaging, oocytes were fixed in 4% PFA for 15 minutes at room temperature following brief (1-2 minute) serial washes in 1% and then 2% PFA. Fixed oocytes were labelled with mouse anti-TUBA (also known as α-tubulin) antibodies (Sigma; 1:9000) followed by anti-mouse IgG Alexa488 conjugate (Molecular Probes; 1:500) and stained with propidium iodide (Sigma). Fluorescence was visualised on a Nikon Eclipse E600 microscope equipped with a Radiance 2100 laser scanning confocal system (BioRad).

Microarray profiling

RNA was recovered from acutely isolated samples using the *mir*Vana miRNA isolation kit (Ambion) and analysed essentially as described previously (Amanai et al., 2006a). Data sets were deposited at the NCBI Gene Expression Omnibus (http://www.ncbi.nlm.nih.gov/projects/geo/) with the series accession number GSE4822.

RESULTS

Native PLCZ1 activity and promoter mapping in transgenic mice

Determining the specificity of PLCZ1 should illuminate its role and mechanism. Mouse *Plcz1* transcripts were present in the testes of post-pubertal males (4 weeks and older) and at low levels in pre- and post-pubertal brains of both sexes (Fig. 1A; data not shown). The identity of brain *Plcz1* was confirmed by sequencing. A narrow expression profile for PLCZ1 (protein) has previously been noted but did not include the brain (Saunders et al., 2002).

To map the promoter elements responsible for this restricted expression, transgenic mice were generated in which genomic DNA fragments 4.5 and 4.1 kb upstream of the putative *Plcz1* translational start codon respectively directed transcription of either a *Cre* or *Plcz1* cassette (Fig. 1B). Each fragment included the *Plcz1* transcriptional start mapped by 5′-RACE (Fig. 1B) (Fujimoto et al., 2004). Transgene (tg) constructs were expressed in the brains of males and females and the testes of males, with a high degree of tissue but not developmental specificity in three out of the five independent lines analysed (see Table S1 in the supplementary material). This suggests that the 4.1 kb *Plcz1* promoter fragment directs spatial, but not temporal, restriction of *Plcz1* expression. In addition to a 67 nucleotide region (5′-CATGTG...ACACAG-3′) of strong Z-DNA potential (Champ et al., 2004), the fragment harbours canonical recognition motifs for sex-

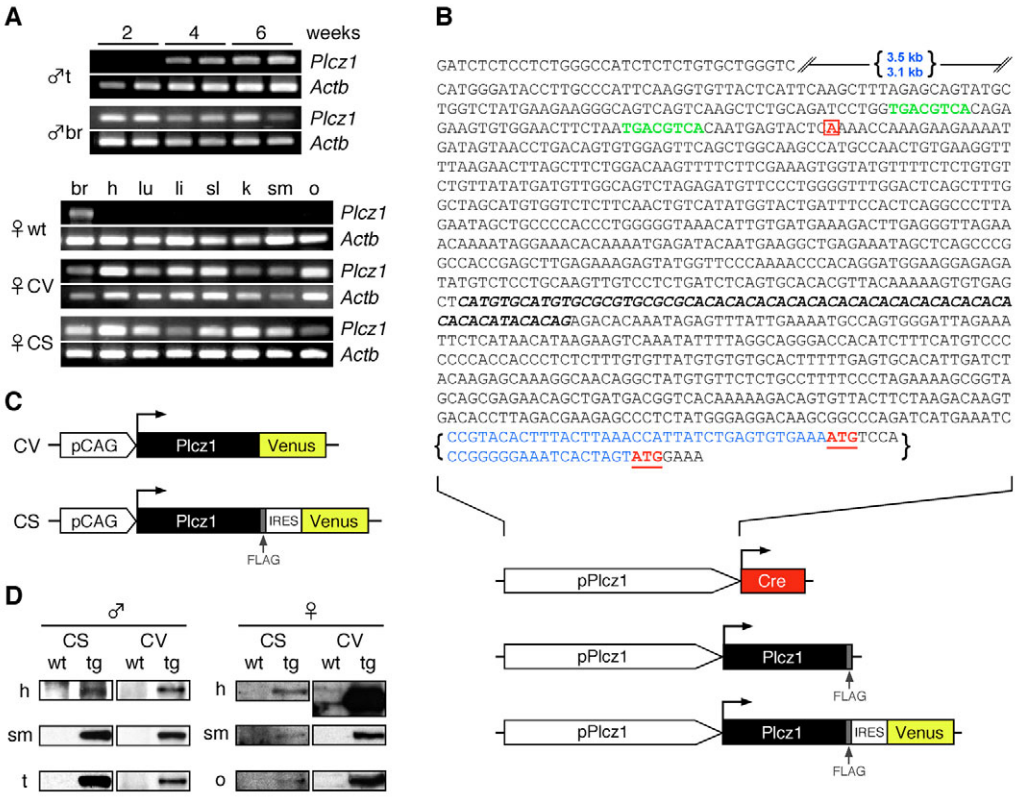

Fig. 1. *Plcz1* expression in wild-type and transgenic mice. (**A**) *Plcz1* RT-PCR on testes (t) and brains (br) from duplicate wild-type males at the ages shown (upper) and from wild-type (wt) and F_2 transgenic females on brain (br), heart (h), lung (lu), liver (li), spleen (sl), kidney (k), skeletal muscle (sm) and ovaries (o) (beneath). (**B**) Configurations of *Plcz1* promoter-mapping constructs with Cre and rPLCZ1 reporters, showing cAMP-responsive element binding protein (CREBP) cognate sequences (green), the putative transcriptional start site (red, boxed), a region of high Z-DNA potential (bold, italicised) and the putative translational start codon (red, underlined). Sequences unique to each construct are indicated in blue, with Cre uppermost. Beneath are shown the structures of downstream open reading frames. (**C**) Structures (not to scale) of CV and CS tg constructs. Arrows mark the start and direction of translation. (**D**) Immunoblotting to show rPLCZ1 and PLCZ1 expression in heart (h), skeletal muscle (sm), testes (t) and ovaries (o) of CS and CV hemizygotes (tg) and aged-matched, non-transgenic littermates (wt).

determining region Y (SRY) protein (Harley et al., 1992) and a perfect repeat of the palindromic cAMP-responsive element binding protein (CREBP; also known as CREB5) cognate sequence (Fig. 1B) (Maekawa et al., 1989). A similar configuration directs thimet oligopeptidase (*Thop1*) gene expression in spermatid-derived cell lines (Morrison and Pierotti, 2003).

PLCZ1 specificity probed with ectopically expressed transgenes

Having verified the native *Plcz1* expression profile, we were able to evaluate the specificity of PLCZ1 by forcing its expression ectopically. A promiscuous promoter was selected to direct broad expression in transgenic lines encoding PLCZ1 either fused to Venus (CV) or whose coding sequence was separated from that of Venus by an *IRES* (CS) (Fig. 1C).

Founder ovarian *Plcz1* transcript levels were quantified (not shown). Adult males and females of lines CV3 and CS16 expressed tg transcripts and recombinant PLCZ1 (rPLCZ1) protein in multiple tissues (Fig. 1D). Protein expression in the CV3 F_1, CV3-13, was higher than that of subsequent outbred generations.

CV3 and CS16 individuals of either sex appeared healthy for the first ~3 months, indicating that PLCZ1 is largely inert at the levels found in these lines. Male hemizygotes outcrossed with C57BL/6 produced litter sizes within the control range (7.91±0.29, n=105, P>0.05), but female CV3 or CS16 hemizygotes crossed with C57BL/6 males produced litter sizes significantly smaller than those of controls (0.85±0.348, n=26, P<0.0001). Such disruption of female reproductive function by rPLCZ1 was consistent with maternal meiotic abnormalities.

Oocytes from PLCZ1-expressing females undergo meiotic maturation to mII, followed by parthenogenetic activation

Immature oocytes collected from *rPlcz1* transgenic females underwent GV breakdown and entered mI before extruding a Pb_1 and forming an mII spindle (Fig. 2A). Time-lapse imaging (see Movie 1 in the supplementary material) showed normal kinetics of Pb_1 extrusion in hemizygotes (P=0.81) en route to mII (Fig. 2A-D); the mean Pb_1 extrusion time for hemizygotes was 12.80±0.42 hours post-collection (n=34 oocytes), and for non-transgenic littermates it was 12.65±0.47 hours (n=24 oocytes). Spindle and chromosome behaviour during maturation were indistinguishable in oocytes from hemizygotes and controls (Fig. 2A). Injection of wild-type GV oocytes with sperm-derived active PLCZ1 (Fujimoto et al., 2004) did not interfere with meiotic progression (n=38). Superovulated oocytes from hemizygotes analysed ~13 hours after human chorionic gonadotropin (hCG) administration possessed an mII plate (Fig. 2A,C,D), a clear Pb_1, condensed metaphase

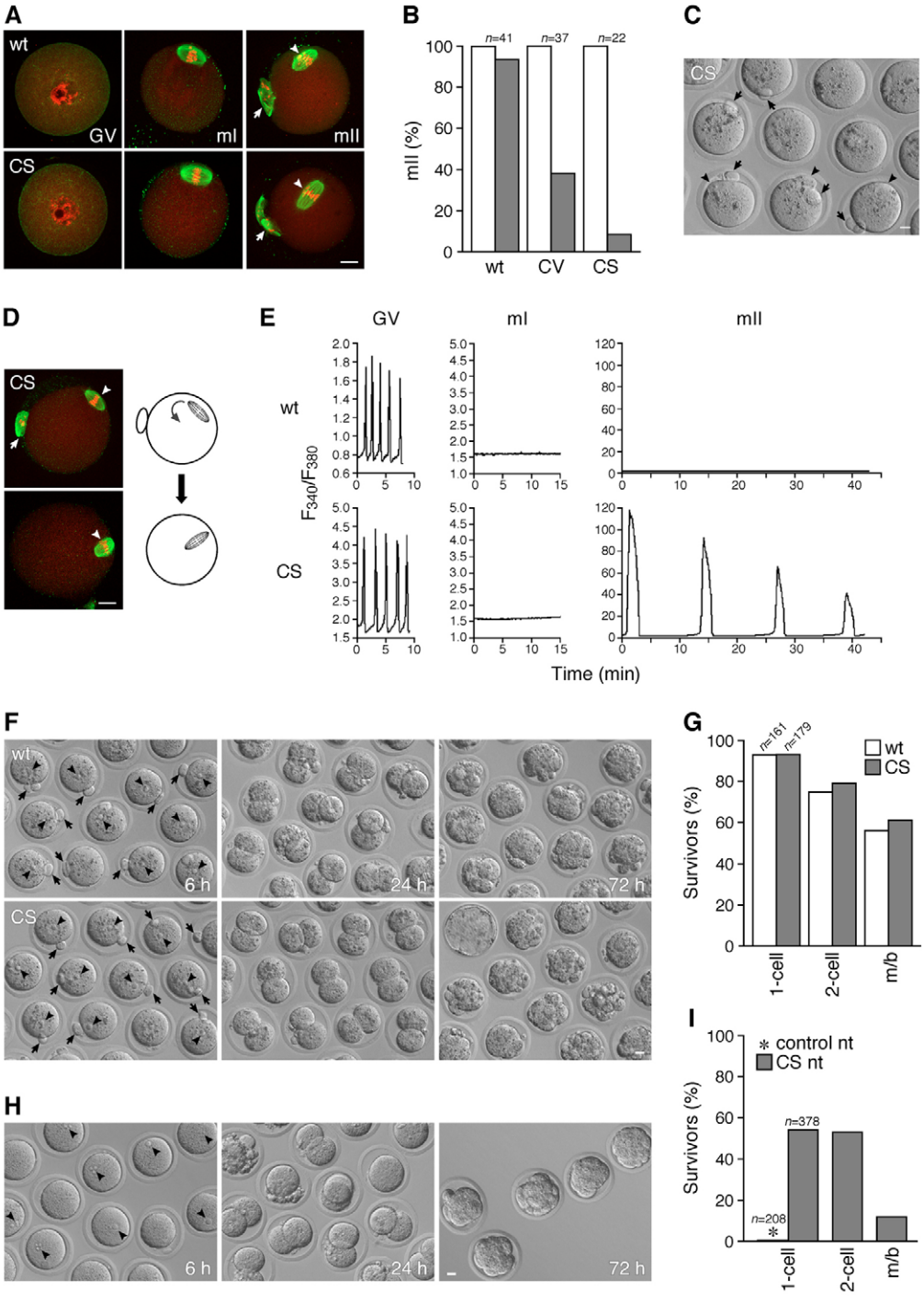

Fig. 2. Parthenogenesis follows normal meiotic progression in rPLCZ1-expressing hemizygous female mice.
(**A**) Immunofluorescence microscopy of oocytes matured in vitro at <2 (GV) or 8-10 (mI) hours after meiotic resumption, or ~13 hours post-hCG (mII). Oocytes were from hemizygotes (CS) and age-matched non-transgenic littermates (wt). TUBA2 labelling is green and genomic DNA red. Arrows and arrowheads respectively mark the first polar body (Pb_1) and mII plate. (**B**) Proportion of age-matched oocytes upon collection at mII ~13 (white) and 24 (grey) hours post-hCG. (**C**) Hofmann image of F_4 oocytes 13.5-14 hours post-hCG, showing metaphase or anaphase-telophase distortions (arrowheads) and Pb_1 (arrows). (**D**) Immunofluorescence microscopy of different oocytes from C, ~14 hours post-hCG, at early (upper) and late (beneath) stages of spindle rotation, represented diagrammatically to the right. Staining and key to arrow and arrowheads are as for A. (**E**) Ratiometric Fura 2-AM $[Ca^{2+}]_i$ imaging of representative oocytes at different stages, performed as for A but with mII oocytes 14.5 hours post-hCG. Oocytes were from non-transgenic control (wt, upper) and age-matched transgenic (CS, beneath) females. (**F**,**G**) Hofmann images (F) and bar chart (G) showing development in vitro of CS16 F_3 (CS) and $SrCl_2$-induced wild-type (wt) haploid parthenogenotes at the times shown after oocyte collection or activation. Pronuclei and Pb_2 in F are respectively indicated with arrowheads and arrows. (**H**) Preimplantation development following nuclear transfer (nt) from CS16 F_4 cumulus cell nuclei into enucleated wild-type oocytes without exogenous activation, shown at the times indicated (hours) post-nt. Pronuclei are indicated with arrowheads. (**I**) Developmental rates in vitro following nt of CS16 F_3 and F_4, or age-matched non-transgenic or *pCAG→mtVenus* transgenic (Shoji et al., 2006) cumulus cells (control) into enucleated wild-type oocytes. m/b (in G,I), morula/blastocyst. Scale bars: 20 μm.

chromosomes attached to spindles and *Fbxo43* mRNA at 99.7±9.8% of control levels (n=6) (Shoji et al., 2006). During maturation, oocytes from transgenic (GV, n=18; mI, n=18) and non-transgenic (GV, n=17; mI, n=18) females exhibited a similar pattern of $[Ca^{2+}]_i$ oscillations (Fig. 2E) reminiscent of that previously described for wild-type oocytes (Carroll et al., 1994). Oscillation amplitudes in GV oocytes from transgenic females were greater than those of controls (Fig. 2E). Although PLCZ1 may boost $[Ca^{2+}]_i$ oscillation amplitude at the GV stage, these findings indicate in different ways that PLCZ1 does not functionally interfere with meiotic maturation and that most, or all, oocytes establish mII in the presence of rPLCZ1.

During or soon after oocyte collection (~13 hours post-hCG), metaphase arrays were observed to rotate and/or separate in preparation for cytokinesis (Sun and Schatten, 2006), indicating meiotic exit (Fig. 2D). Collected oocytes exhibited spontaneous

$[Ca^{2+}]_i$ rises of variable (and often very large) amplitude with first-to-second recorded peak intervals of 12.48±0.82 minutes (n=16) initiated by a basal pacemaker rise characteristic of fertilisation (Jones et al., 1995; Perry et al., 2000) (Fig. 2E). Parthenogenotes emitted a Pb_2, formed a single maternal pronucleus of normal size and developed efficiently to the morula/blastocyst stage in vitro (Fig. 2F,G).

It is possible that rPLCZ1 expression during meiotic maturation abrogated the installation of one or more activities needed to sustain mII arrest, rather than by inducing mII exit as at fertilisation. We evaluated this by transferring the nuclei of transgenic cumulus cells (which contain *rPlcz1* mRNA, not shown) into wild-type mII oocytes. Nuclear transfer induced pronuclear activation in ~60% of cases; this level approximates to the proportion of oocytes activated by 1.25 fg of sperm-derived PLCZ1 (50%) (Fujimoto et al., 2004), suggesting that a similar amount of rPLCZ1 was transferred with each cumulus cell nucleus. Nuclear transfer zygotes cleaved efficiently and developed in vitro (Fig. 2H,I). Thus, rPLCZ1 produced in vivo directly stimulates the parthenogenetic activation of mII oocytes.

The level of *rPlcz1* mRNA in mature mII oocytes from hemizygotes was only 12.3±11.3% of that of GV oocytes (n=8, P=0.0001). Consistent with this, maturing ovarian (but not mII) oocytes of the line CS16 exhibited clear Venus epifluorescence (Fig. 3A); Venus is encoded by the same bicistronic mRNA as rPLCZ1 in the line CS16 (Fig. 1C). This suggests that meiotic exit was induced by PLCZ1 that had been produced prior to mII.

Oviductal parthenogenotes at later cleavage stages, including blastocysts, were recovered from transgenic females 16 hours post-hCG (Fig. 3B), showing that activation occurred independently of superovulation.

Highly penetrant ovarian tumourigenesis in PLCZ1 transgenic females

Hemizygous CS16 and CV3 ovaries were typically of healthy appearance at 3-4 months. However, histochemical sectioning of one intact transgenic ovary revealed an early-stage follicular choriocarcinoma or yolk sac tumour (Fig. 3C).

Most young rPLCZ1-expressing individuals were overtly asymptomatic, but by 5-6 months, many females had developed abdominal swellings caused by ovarian tumours (Fig. 4A). Tumourigenesis exhibited a typical latency of ⩾3 months, although onset was apparent macroscopically as early as 61 days. Age-matched rPLCZ1-expressing males remained largely asymptomatic. Tumour formation in females was highly penetrant (Fig. 4B) and occurred bilaterally or unilaterally (Fig. 4A). Hemizygous females occasionally (14.7%, n=116) contained abortive implantation fossa (Fig. 4C) without evidence of uterine tumourigenesis. Development of ovarian tumours was also highly penetrant in ICR outcrosses; 92.9% of females from ICR×CS16 crosses developed tumours (n=14). Tumour development was therefore not highly restricted by genetic background.

The *rPlcz1* tg integrant dosage in most (69%, n=13) tumours was generally ~1.0-1.5 per diploid genome complement as determined by qPCR (Fig. 4D). Apparent tg dosages were generally conserved even when genomic DNA samples were taken from multiple (up to six) sites in the same growth (Fig. 4D) and thus did not reflect an averaging of 0.0 and 2.0 integrations per genome across the entirety of a given tumour.

Tumours contained elevated levels of *rPlcz1* mRNA relative to controls (P=0.0046) and decreased levels of *Mos* and *Fbxo43* transcripts (P⩽0.00023), which are downregulated post-activation

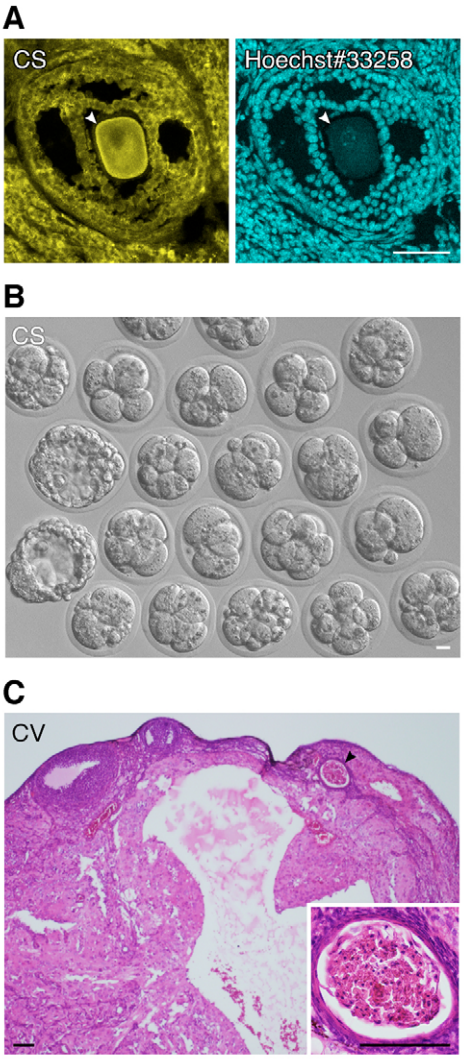

Fig. 3. Timing and early in vivo consequences of rPLCZ1 expression. (**A**) Epifluorescence microscopy of mouse ovarian follicle section showing Venus expression (left) within a maturing primary oocyte (arrowhead), stained for DNA (right). (**B**) Asynchronous parthenogenotes recovered from hemizygotes 16 hours post-hCG. (**C**) Hematoxylin and Eosin staining of an 11-week-old hemizygous ovary which appeared macroscopically normal, at low and higher (inset) magnification, showing a nascent follicular choriocarcinoma or yolk sac tumour. Scale bars: 50 μm in A,C; 20 μm in B.

(Fig. 5A) (Shoji et al., 2006). Whereas miRNA profiles are the signatures of some solid tumours (Lu et al., 2005; Volinia et al., 2006), the profiles of teratomas were diverse, reflecting teratoma heterogeneity (see Fig. S1 in the supplementary material).

Imprinted gene expression in tumours was found to be segregated, with paternally-expressed transcripts present at significantly lower levels (P<0.05 for seven out of the ten genes examined) than in controls, whereas steady-state levels of seven out of nine maternally-expressed mRNAs were ~1.0 or >1.0 compared with controls (Fig. 5B). Transcripts for placental markers *Plac1*, *Gcm1*, *Zfp36l3*, *Plib* and *Tpbpa* (Fig. 5C) were not detected. These profiles are expected for parthenogenetic tumours in which paternally imprinted alleles and placental tissue are depleted or absent.

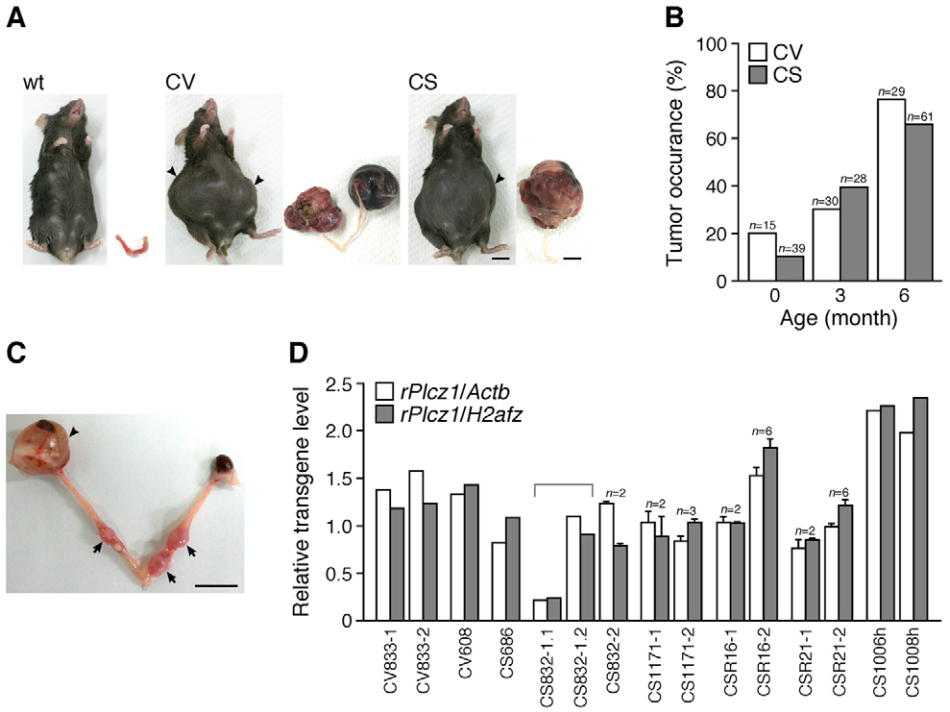

Fig. 4. Ovarian tumours in PLCZ1-expressing female mice.
(**A**) Hemizygous F_2 CV3 and CS16 females at ~6 months, with age-matched control (wt) showing abdominal distensions (arrowheads) and the tumours that caused them. (**B**) Percentages of transgenic females with tumours at the ages shown. (**C**) Reproductive tissue from a hemizygote at ~6 months with a small tumour (arrowhead) and three regressing implantation fossa (arrows). (**D**) Dosages of tgs (*rPlcz1*) determined for 12 ovarian tumours relative to levels of the native genes *Actb* and *H2afz*. All tumours were from hemizygous females. Somatic tissue from homozygotes (CS1006h and CS1008h) gave expected tg dosages of ~2. Error bars (±s.e.m.) were produced from results obtained for different (*n*) samples from the same tumour. Discrete portions from the tumour CS832-1 (bracketed) possessed disparate relative tg dosages. Scale bars: 1 cm.

Histopathology of tumours at 4-6 months revealed mature cystic teratoma (epidermoid cyst), cystadenoma with borderline malignancy, and mixed germ cell tumours (Fig. 6). Histological heterogeneity reflects the extensive capacity for multipotent differentiation of parthenogenetic lineages (Stevens, 1978). The presence of mature cystic teratoma may represent remnants of incompletely regressed Wolfian duct, and cystadenomas are also found in aging mice, either of which might be due to somatic cell differentiation. However, we never observed ovarian tumours in age-matched, non-transgenic littermates.

The appearance of dysgerminoma, yolk sac tumourigenesis and choriocarcinoma characterise the differentiation of pluripotent embryonic or germ cells. The predominance and frequency of such tumours provide a clear causal link between PLCZ1-induced parthenogenesis and tumourigenesis.

The relationship between PLCZ1 expression, ataxia and different contexts of ovarian tumourigenesis

We addressed the possibility that LT/Sv oocytes contain active PLCZ1. With the exception of the brain, a site of wild-type *Plcz1* expression (Fig. 1A), *Plcz1* transcript levels in other female LT/Sv tissues (including ovaries) at 8 weeks were undetectable (Fig. 5D). We verified this result by sequencing the 4.5 kb *Plcz1* promoter region (Fig. 1B) of LT/Sv and that of its presumptive relative, the non-parthenogenetic strain BALB/c (Eppig et al., 1996); the sequences were identical (not shown). Promoter sequence conservation and the lack of ovarian *Plcz1* mRNA indicate that LT/Sv phenotypes are not due to anomalous *Plcz1* expression.

rPlcz1 transgenic mice exhibited occasional (*n*=7) hind limb ataxia (see Movie 2 in the supplementary material). The high-level expresser, CV3-13, was ataxic and although no CS16 hemizygotes exhibited the phenotype, two homozygotes did. Of the remaining four affected members of the CV3 line, two were male and two female. These data show that the phenotype was not sex-specific and may correlate with PLCZ1 expression levels.

Some cases of human ovarian cancer also present with ataxia (Geomini et al., 2001). We investigated whether human tumours contained elevated levels of *PLCZ1* mRNA in common with the tumours of CV3 and CS16 lines (not shown). However, we found no evidence for genetically predisposed *PLCZ1* expression in human breast epithelial (*n*=15), or ovarian epithelial (*n*=15) or benign ovarian germline (*n*=22) tumours (Fig. 5E and not shown).

DISCUSSION

The implications of developmental specificity for the mechanism of PLCZ1

The developmental specificity of PLCZ1 is highlighted by its narrow wild-type expression profile and the restriction of its activity to oocytes (and possibly brain) when low-level expression is forced ectopically in multiple tissues.

The principal phenotypes induced by *rPlcz1* tg expression – parthenogenesis, tumourigenesis and, to a lesser extent, ataxia in both sexes – are thus apparently associated with those tissues in which *Plcz1* is normally expressed (Fig. 1A). This argues that the cellular machinery required to transduce PLCZ1 signalling is restricted to the same tissues: oocytes and the brain. Our preliminary data suggest that within the brain, *Plcz1* mRNA is predominantly localised to the telencephalon (not shown). In one model, the presence of telencephalic PLCZ1 signal-transducing machinery would render the telencephalon susceptible to PLCZ1 overexpression, resulting in motor function defects that account for sporadic ataxia. A plausible role for this machinery (and its counterpart in the oocyte) would be to facilitate the targeting of PLCZ1 to PIP_2 (as its C2 domain is insufficient to do so) in a manner similar to the interaction of PLCB1 with GNAQ (Wang et al., 1999; Kouchi et al., 2005). The possibility remains open that

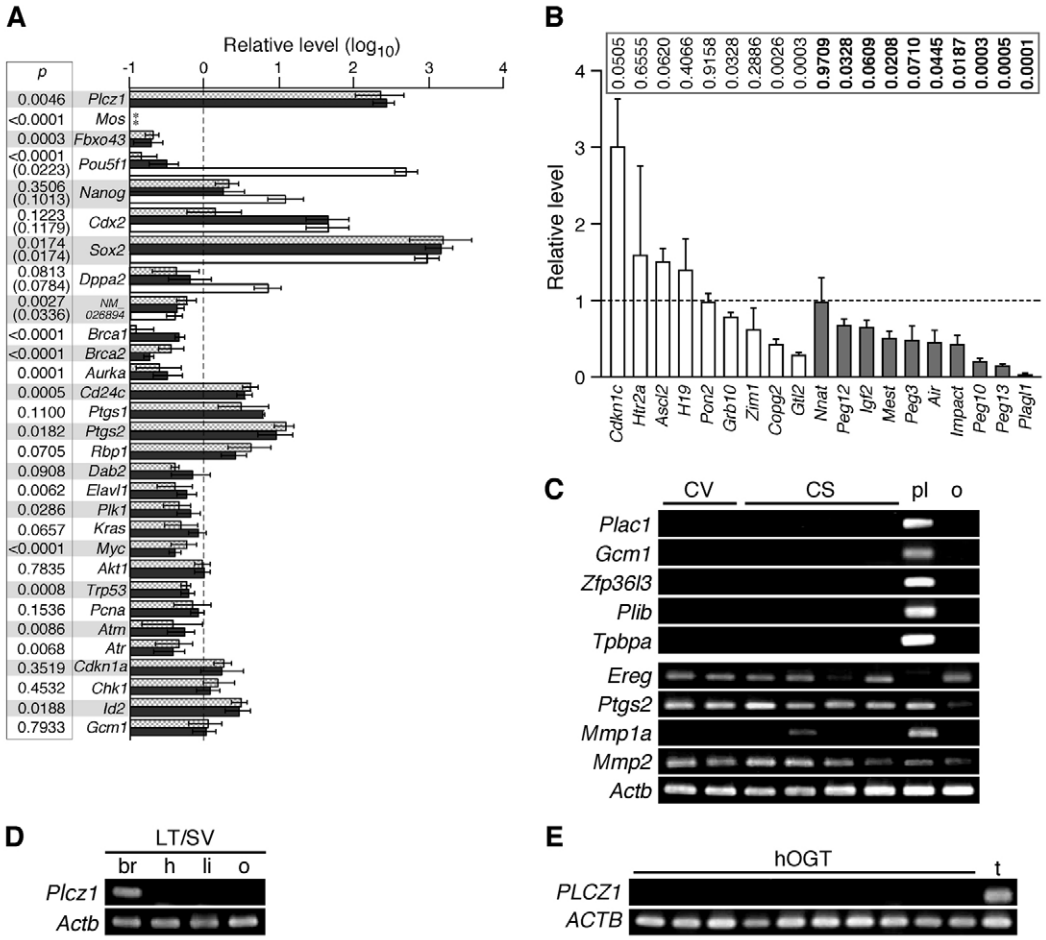

Fig. 5. *Plcz1* expression in tumours and in the tumourigenic strain LT/Sv, and expression of its human orthologue in tumours. (**A**) Relative mRNA levels determined by qPCR for tumours from CV3 (stippled) and CS16 (grey) relative to wild-type ovary, or combined and expressed relative to skeletal muscle (white). Error bars, ±s.e.m.; *, not detected. Corresponding *P*-values are shown for unpaired Student's *t*-tests. (**B**) Tumour transcript levels of maternally- (white) and paternally- (grey) expressed imprinted genes determined by qPCR and represented relative to respective levels in wild-type ovary (1.0). Error bars, ±s.e.m. *P*-values (above), unpaired Student's *t*-tests. (**C**) RT-PCR analysis of two CV3 (CV) and four CS16 (CS) tumours, wild-type placenta (pl) and ovaries (o), for placental marker and metastasis-associated gene expression. (**D**) RT-PCR (35 cycles) of selected tissues from an 8-week-old LT/Sv female. Key as per Fig. 1. (**E**) RT-PCR for *PLCZ1* and control *ACTB* mRNAs in ten independent human ovarian germline tumour (hOGT) biopsy samples as indicated. t, mouse testis control.

higher levels of ectopic PLCZ1 expression overcome the requirement for an adaptor to induce broader (lethal) embryonic phenotypes not investigated here.

Although PLCZ1 is normally expressed in the testis, we did not find evidence of abnormal cellular proliferation in the testes of transgenic males. This could be because tg expression did not significantly augment the total level of PLCZ1 (relative to native PLCZ1) and/or because the testis also lacks PLCZ1 signal-transducing machinery. A downstream target of PLCZ1 signalling in oocytes, FBXO43, is abundant in, and exclusive to, the testis in adult males (Shoji et al., 2006). Teratomas in males are more likely to be malignant than those in females (Stevens, 1967), so although a male meiotic role for FBXO43 is presumptive, PLCZ1-FBXO43 signalling in the testis could perturb the cell cycle and result in catastrophic neoplastic germ cell transformation, implying the stringent need to avoid it.

In summary, the data presented here suggest that PLCZ1 activity in vivo requires tissue-specific accessory factors. These might include adaptors that bind to PLCZ1, thereby compensating for its inherent lack of PH or SH domains.

PLCZ1-induced parthenogenesis and its relationship to other in vivo models of parthenogenesis

Several lines of evidence suggest that oocytes in *rPlcz1* transgenic lines CV3 and CS16 complete meiotic maturation before undergoing activation. Ectopic rPLCZ1 expression during oogenesis thus represents the first in vivo model in which the normal program of coordinated maternal cytoplasmic and nuclear maturation precedes autonomous parthenogenetic activation.

Endogenous expression from *rPlcz1* tgs induced meiotic exit in a manner characteristic of normal fertilisation. Demonstration of this faculty in vivo circumvents some drawbacks of injection experiments, which do not completely eliminate the possibility that non-physiological RNA or exogenous impurities act as co-factors; enzymes such as telomerase have an RNA component (Greider and Blackburn, 1987) and non-DNA-metabolising signalling enzymes such as DNA protein kinase require DNA (Carter et al., 1990).

Parthenogenesis occurs in both *Mos*-deficient and LT/Sv oocytes. In the absence of MOS, MAPK signalling is not established during mI (Araki et al., 1996; Choi et al., 1996). LT/Sv

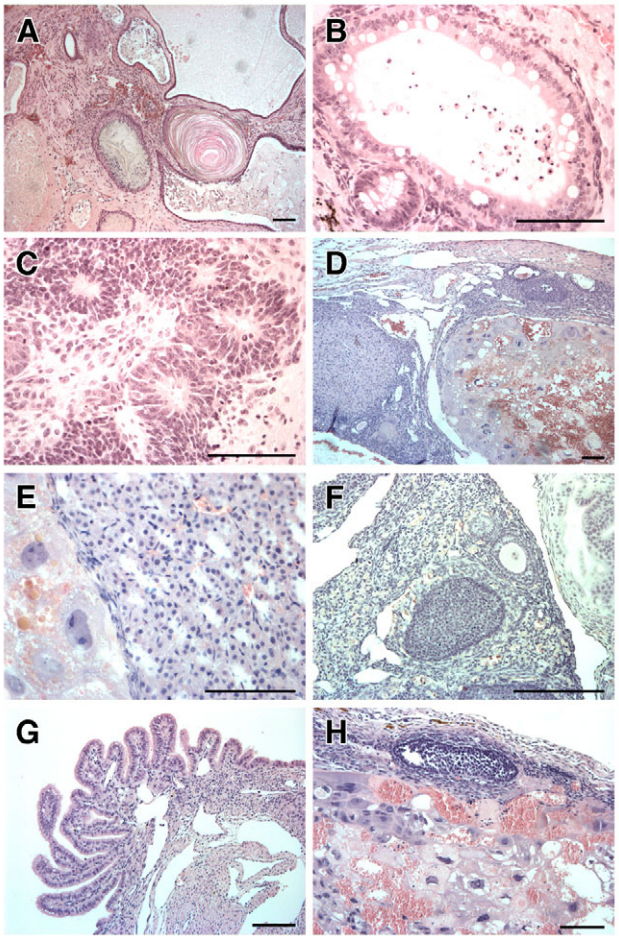

Fig. 6. Histopathology of rPLCZ1-induced ovarian tumours. (**A**) Mature cystic teratoma (epidermoid cyst) with keratinisation. (**B**) Intestinal epithelium with goblet cells. (**C**) Neurectodermal rosettes with tubules and glia-like stroma. (**D**) Mixed germ cell tumour showing yolk sac tumour (right), choriocarcinoma (top) and dysgerminoma (left). (**E**) Dysgerminoma (right) with yolk sac tumour. (**F**) Nests of dysgerminoma cells with follicle. (**G**) Mucinous cystadenoma with borderline malignancy of columnar epithelium. (**H**) Mixed germ cell tumour showing yolk sac tumour (right) and choriocarcinoma (top). Sections stained with Hematoxylin and Eosin are from three CV3 (A-E) and two CS16 (F-H) F_2 female mice. Scale bars: 100 μm.

oocytes frequently arrest at mI (Hampl and Eppig, 1995); this failure is associated with precocious cell cycle progression but is not sufficient to induce it (Eppig et al., 1996). LT/Sv females heterozygous for the polymorphic marker *Gpi1* produce homozygous tumours and, although it was inferred from this that the teratomas arose from oocytes that completed meiosis I (Eppig et al., 1977), reductive division of tetraploid cells at any stage in early tumourigenesis, followed by clonal selection (or other pathways), could produce the same result. Moreover, tumour cells of *rPlcz1* transgenic mice are apparently hemizygous. Finally, LT/Sv oocytes efficiently induce activation when fused to wild-type mII oocytes (Ciemerych and Kubiak, 1998), yet this is not owing to expression of PLCZ1 (Fig. 5D). Previous in vivo models of parthenogenesis reflect aberrant mI and differ from the one described here.

The link between parthenogenesis and tumour formation

In one mechanistic model linking parthenogenesis in vivo to tumourigenesis, PLCZ1 activates mII oocytes that fail to be released from their ovarian environment, resulting in quasi-embryonic growth to form a teratoma. Histopathology and the patterns of imprinted and placental gene expression corroborate the parthenogenetic provenance of the tumours, but this model is simplistic.

The model does not explain the apparent hemizygosity of most tumours within hemizygous females, as the clonal generation of diploid cells from haploid parthenogenotes (Kaufman et al., 1983) would generally result in homozygosity [as it does in LT/Sv, where tumours arise from meiosis I failure and are homozygous in ~90% of cases (Eppig et al., 1977)]. This objection is addressed if a primary tumour in rPLCZ1-expressing females impeded subsequent ovulation, thereby increasing the likelihood of supernumerary tumours in the same ovary and enabling the fusion of the cells of different early teratomas. Tumour cells generally (but not always) contained the *rPlcz1* tg, implying a post-activation selective advantage of PLCZ1 expression.

Tumourigenesis could have followed failure of meiosis I and subsequent cytoplasmic maturation, allowing activation by rPLCZ1 of an oocyte containing four genomic complements (Mehlmann and Kline, 1994; Carroll et al., 1996). We found no evidence to support this model and several observations argue against it. PLCZ1 expression did not interfere with oocyte maturation (Fig. 2A-E and see Movie 1 in the supplementary material), and even where parthenogenesis due to the failure of meiosis I occurs at high frequency [~100% in the case of *Mos*-null oocytes (Colledge et al., 1994)], the frequency of tumour formation is markedly lower: 30% for *Mos*-null mice versus ⩾60% for ectopic rPLCZ1 expression (Furuta et al., 1995) (Fig. 4B). Parthenogenesis in LT/Sv is not sufficient to induce tumour formation (Eppig et al., 1996) and the genotype predisposing to the LT/Sv phenotype maps to at least three unascribed loci (Lee et al., 1997; Everett et al., 2004), none of which is *Plcz1* (Fig. 5D).

Although wild-type parthenogenotes exhibit retarded extra-embryonic development, they are able to develop for ~10 days in vivo (Kaufman et al., 1977) and, in keeping with this, we observed uterine implantation in transgenic virgins (Fig. 4C). Implantation can occur ectopically (McLaren and Tarkowski, 1963) and embryonal carcinoma cells generate tumours in vivo (Stevens, 1970). The ovary is clearly not a unique niche for teratoma development and the failure of uterine tumours to develop suggests either that growth was too slow or that uterine mechanisms exist to prevent parthenogenic tumour development.

We found no evidence of metastasis in rPLCZ1-expressing mice, although the pronounced growth of ovarian tumours indicated angiogenesis (Folkman and Klagsbrun, 1987) and at least one tumour from the CS line (Fig. 5C) expressed all four signature genes (*Ereg*, *Ptgs2*, *Mmp1a* and *Mmp2*) for lung tumourigenesis and metastasis (Gupta et al., 2007). We were unable to detect expression of the cancer stem cell marker protein PROM1 (CD133) (Hemmati et al., 2003) immunohistochemically in teratomas (not shown). Although this suggests that in general, cell fate commitment was an early event in ovarian tumour establishment (Avilion et al., 2003; Kania et al., 2005), the presence of *NM_026894* and *Pou5f1* transcripts in tumours (Fig. 5A) is consistent with a small population of relatively undifferentiated cells (Monk and Holding, 2001; Tai et al., 2005).

These data collectively demonstrate that oocytes exposed to endogenous PLCZ1 mature normally and establish mII. PLCZ1 is sufficient to induce meiotic exit, parthenogenetic development and teratoma formation with exquisite specificity. The studies establish a novel relationship between fertilisation and tumourigenesis and imply a tractable model with which to study the dysregulation (and thereby the productive orchestration) of embryogenesis.

We are grateful to Dr Joe Xhou of LC Sciences for miRNA analysis, to Satoko Fujimoto for assistance with western blotting, to the Laboratory of Animal Resources and Genetic Engineering for their unsung heroism and to Dr Kazuhiro Kitada for the generous provision of LT/Sv mice.

Supplementary material

Supplementary material for this article is available at http://dev.biologists.org/cgi/content/full/134/21/3941/DC1

References

Amanai, M., Brahmajosyula, M. and Perry, A. C. F. (2006a). A restricted role for sperm-borne microRNAs in mammalian fertilization. *Biol. Reprod*. **75**, 877-884.

Amanai, M., Shoji, S., Yoshida, N., Brahmajosyula, M. and Perry, A. C. F. (2006b). Injection of mammalian metaphase II oocytes with short interfering RNAs to dissect meiotic and early mitotic events. *Biol. Reprod*. **75**, 891-898.

Araki, K., Naito, K., Haraguchi, S., Suzuki, R., Yokoyama, M., Inoue, M., Aizawa, S., Toyoda, Y. and Sato, E. (1996). Meiotic abnormalities of *c-mos* knockout mouse oocytes: activation after first meiosis or entrance into third meiotic metaphase. *Biol. Reprod*. **55**, 1315-1324.

Avilion, A. A., Nicolis, S. K., Pevny, L. H., Perez, L., Vivian, N. and Lovell-Badge, R. (2003). Multipotent cell lineages in early mouse development depend on SOX2 function. *Genes Dev*. **17**, 126-140.

Carroll, J., Swann, K., Whittingham, D. and Whitaker, M. (1994). Spatiotemporal dynamics of intracellular $[Ca^{2+}]$i oscillations during the growth and meiotic maturation of mouse oocytes. *Development* **120**, 3507-3517.

Carroll, J., Jones, K. T. and Whittingham, D. G. (1996). Ca^{2+} release and the development of Ca^{2+} release mechanisms during oocyte maturation: a prelude to fertilization. *Rev. Reprod*. **1**, 137-143.

Carter, T., Vancurova, I., Sun, I., Lou, W. and DeLeon, S. (1990). A DNA-activated protein kinase from HeLa cell nuclei. *Mol. Cell. Biol*. **10**, 6460-6471.

Champ, P. C., Maurice, S., Vargason, J. M., Camp, T. and Ho, P. S. (2004). Distributions of Z-DNA and nuclear factor I in human chromosome 22, a model for coupled transcriptional regulation. *Nucleic Acids Res*. **32**, 6501-6510.

Choi, T., Fukasawa, K., Zhou, R., Tessarollo, L., Borror, K., Resau, J. and Vande Woude, G. F. (1996). The Mos/mitogen-activated protein kinase (MAPK) pathway regulates the size and degradation of the first polar body in maturing mouse oocytes. *Proc. Natl. Acad. Sci. USA* **93**, 7032-7035.

Ciemerych, M. A. and Kubiak, J. Z. (1998). Cytostatic activity develops during meiosis I in oocytes of LT/Sv mice. *Dev. Biol*. **200**, 198-211.

Colledge, W. H., Carlton, M. B., Udy, G. B. and Evans, M. J. (1994). Disruption of c-*mos* causes parthenogenetic development of unfertilized mouse eggs. *Nature* **370**, 65-68.

Cuthbertson, K. S. R. (1983). Parthenogenetic activation of mouse oocytes in vitro with ethanol and benzyl alcohol. *J. Exp. Zool*. **226**, 311-314.

Eppig, J. J., Kozak, L. P., Eicher, E. M. and Stevens, L. C. (1977). Ovarian teratomas in mice are derived from oocytes that have completed the first meiotic division. *Nature* **269**, 517-518.

Eppig, J. J., Wigglesworth, K., Varnum, D. S. and Nadeau, J. H. (1996). Genetic regulation of traits essential for spontaneous ovarian teratocarcinogenesis in strain LT/Sv mice: aberrant meiotic cell cycle, oocyte activation, and parthenogenetic development. *Cancer Res*. **56**, 5047-5054.

Everett, C. A., Auchincloss, C. A., Kaufman, M. H., Abbott, C. M. and West, J. D. (2004). Genetic influences on ovulation of primary oocytes in LT/Sv strain mice. *Reproduction* **128**, 565-571.

Folkman, J. and Klagsbrun, M. (1987). Angiogenic factors. *Science* **235**, 442-447.

Fujimoto, S., Yoshida, N., Fukui, T., Amanai, M., Isobe, T., Itagaki, C., Izumi, T. and Perry, A. C. F. (2004). Mammalian phospholipase Cζ induces oocyte activation from the sperm perinuclear matrix. *Dev. Biol*. **274**, 370-383.

Furuta, Y., Shigetani, Y., Takeda, N., Iwasaki, K., Ikawa, Y. and Aizawa, S. (1995). Ovarian teratomas in mice lacking the protooncogene c-*mos*. *Jpn. J. Cancer Res*. **86**, 540-545.

Geomini, P. M., Dellemijn, P. L. and Bremer, G. L. (2001). Paraneoplastic cerebellar degeneration: neurological symptoms pointing to occult ovarian cancer. *Gynecol. Obstet. Invest*. **52**, 145-146.

Greider, C. W. and Blackburn, E. H. (1987). The telomere terminal transferase of Tetrahymena is a ribonucleoprotein enzyme with two kinds of primer specificity. *Cell* **51**, 887-898.

Gupta, G. P., Nguyen, D. X., Chiang, A. C., Bos, P. D., Kim, J. Y., Nadal, C., Gomis, R. R., Manova-Todorova, K. and Massague, J. (2007). Mediators of vascular remodelling co-opted for sequential steps in lung metastasis. *Nature* **446**, 765-770.

Hampl, A. and Eppig, J. J. (1995). Analysis of the mechanism(s) of metaphase I arrest in maturing mouse oocytes. *Development* **121**, 925-933.

Harley, V. R., Jackson, D. I., Hextall, P. J., Hawkins, J. R., Berkovitz, G. D., Sockanathan, S., Lovell-Badge. R. and Goodfellow, P. N. (1992). DNA binding activity of recombinant SRY from normal males and XY females. *Science* **255**, 453-456.

Hemmati, H. D., Nakano, I., Lazareff, J. A., Masterman-Smith, M., Geschwind, D. H., Bronner-Fraser, M. and Kornblum, H. I. (2003). Cancerous stem cells can arise from pediatric brain tumors. *Proc. Natl. Acad. Sci. USA* **100**, 15178-15183.

Jones, K. T., Carroll, J. and Whittingham, D. G. (1995). Ionomycin, thapsigargin, ryanodine, and sperm induced Ca^{2+} release increase during meiotic maturation of mouse oocytes. *J. Biol. Chem*. **270**, 6671-6677.

Kania, G., Corbeil, D., Fuchs, J., Tarasov, K. V., Blyszczuk, P., Huttner, W. B., Boheler, K. R. and Wobus, A. M. (2005). Somatic stem cell marker prominin-1/CD133 is expressed in embryonic stem cell-derived progenitors. *Stem Cells* **23**, 791-804.

Kaufman, M. H., Barton, S. C. and Surani, M. A. (1977). Normal postimplantation development of mouse parthenogenetic embryos to the forelimb bud stage. *Nature* **265**, 53-55.

Kaufman, M. H., Robertson, E. J., Handyside, A. H. and Evans, M. J. (1983). Establishment of pluripotential cell lines from haploid mouse embryos. *J. Embryol. Exp. Morphol*. **73**, 249-261.

Kouchi, Z., Fukami, K., Shikano, T., Oda, S., Nakamura, Y., Takenawa, T. and Miyazaki, S. (2004). Recombinant phospholipase Cζ has high Ca^{2+} sensitivity and induces Ca^{2+} oscillations in mouse eggs. *J. Biol. Chem*. **279**, 10408-10412.

Kouchi, Z., Shikano, T., Nakamura, Y., Shirakawa, H., Fukami, K. and Miyazaki, S. (2005). The role of EF-hand domains and C2 domain in regulation of enzymatic activity of phospholipase Cζ. *J. Biol. Chem*. **280**, 21015-21021.

Lawrence, Y., Whitaker, M. and Swann, K. (1997). Sperm-egg fusion is the prelude to the initial Ca^{2+} increase at fertilization in the mouse. *Development* **124**, 233-241.

Lee, G. H., Bugni, J. M., Obata, M., Nishimori, H., Ogawa, K. and Drinkwater, N. R. (1997). Genetic dissection of susceptibility to murine ovarian teratomas that originate from parthenogenetic oocytes. *Cancer Res*. **57**, 590-593.

Lorca, T., Cruzalegui, F. H., Fesquet, D., Cavadore, J. C., Mery, J., Means, A. and Doree, M. (1993). Calmodulin-dependent protein kinase II mediates inactivation of MPF and CSF upon fertilization of *Xenopus* eggs. *Nature* **366**, 270-273.

Lu, J., Getz, G., Miska, E. A., Alvarez-Saavedra, E., Lamb, J., Peck, D., Sweet-Cordero, A., Ebert, B. L., Mak, R. H., Ferrando, A. A. et al. (2005). MicroRNA expression profiles classify human cancers. *Nature* **435**, 834-838.

Maekawa, T., Sakura, H., Kanei-Ishii, C., Sudo, T., Yoshimura, T., Fujisawa, J., Yoshida, M. and Ishii, S. (1989). Leucine zipper structure of the protein CRE-BP1 binding to the cyclic AMP response element in brain. *EMBO J*. **8**, 2023-2028.

Manandhar, G. and Toshimori, K. (2003). Fate of postacrosomal perinuclear theca recognized by monoclonal antibody MN13 after sperm head microinjection and its role in oocyte activation in mice. *Biol. Reprod*. **68**, 655-663.

McLaren, A. and Tarkowski, A. K. (1963). Implantation of mouse eggs in the peritoneal cavity. *J. Reprod. Fertil*. **6**, 385-392.

Mehlmann, L. M. and Kline, D. (1994). Regulation of intracellular calcium in the mouse egg: calcium release in response to sperm or inositol trisphosphate is enhanced after meiotic maturation. *Biol. Reprod*. **51**, 1088-1098.

Monk, M. and Holding, C. (2001). Human embryonic genes re-expressed in cancer cells. *Oncogene* **20**, 8085-8091.

Morrison, L. S. and Pierotti, A. R. (2003). Thimet oligopeptidase expression is differentially regulated in neuroendocrine and spermatid cell lines by transcription factor binding to SRY (sex-determining region Y), CAAT and CREB (cAMP-response-element-binding protein) promoter consensus sequences. *Biochem. J*. **376**, 89-197.

Ozil, J. P., Banrezes, B., Toth, S., Pan, H. and Schultz, R. M. (2006). Ca^{2+} oscillatory pattern in fertilized mouse eggs affects gene expression and development to term. *Dev. Biol*. **300**, 534-544.

Perry, A. C. F., Wakayama, T., Kishikawa, H., Kasai, T., Okabe, M., Toyoda, Y. and Yanagimachi, R. (1999a). Mammalian transgenesis by intracytoplasmic sperm injection. *Science* **284**, 1180-1183.

Perry, A. C. F., Wakayama, T. and Yanagimachi, R. (1999b). A novel *trans*-complementation assay suggests full mammalian oocyte activation is coordinately initiated by multiple, submembrane sperm compartments. *Biol. Reprod*. **60**, 747-755.

Perry, A. C. F., Wakayama, T., Cooke, I. M. and Yanagimachi, R. (2000). Mammalian oocyte activation by the synergistic action of discrete sperm head components: induction of calcium transients and involvement of proteolysis. *Dev. Biol*. **217**, 386-393.

Rauh, N. R., Schmidt, A., Bormann, J., Nigg, E. A. and Mayer, T. U. (2005).

Calcium triggers exit from meiosis II by targeting the APC/C inhibitor XErp1 for degradation. *Nature* **437**, 1048-1052.
Runft, L. L., Jaffe, L. A. and Mehlmann, L. M. (2002). Egg activation at fertilization: where it all begins. *Dev. Biol*. **245**, 237-254.
Saunders, C. M., Larman, M. G., Parrington, J., Cox, L. J., Royse, J., Blayney, L. M., Swann, K. and Lai, F. A. (2002). PLCζ: a sperm-specific trigger of Ca^{2+} oscillations in eggs and embryo development. *Development* **129**, 3533-3544.
Shoji, S., Yoshida, N., Amanai, M., Ohgishi, M., Fukui, T., Fujimoto, S., Nakano, Y., Kajikawa, E. and Perry, A. C. F. (2006). Mammalian Emi2 mediates cytostatic arrest and transduces the signal for meiotic exit via Cdc20. *EMBO J*. **25**, 834-845.
Stevens, L. C. (1967). The biology of teratomas. *Adv. Morphog.* **6**, 1-31.
Stevens, L. C. (1970). The development of transplantable teratocarcinomas from intratesticular grafts of pre- and postimplantation mouse embryos. *Dev. Biol*. **21**, 364-382.
Stevens, L. C. (1978). Totipotent cells of parthenogenetic origin in a chimaeric mouse. *Nature* **276**, 266-267.
Stevens, L. C. and Varnum, D. S. (1974). The development of teratomas from parthenogenetically activated ovarian mouse eggs. *Dev. Biol*. **37**, 369-380.
Sun, Q. Y. and Schatten, H. (2006). Regulation of dynamic events by microfilaments during oocyte maturation and fertilization. *Reproduction* **131**, 193-205.
Sutovsky, P., Manandhar, G., Wu, A. and Oko, R. (2003). Interactions of sperm perinuclear theca with the oocyte: implications for oocyte activation, anti-polyspermy defense, and assisted reproduction. *Microsc. Res. Tech*. **61**, 362-378.
Tai, M. H., Chang, C. C., Kiupel, M., Webster, J. D., Olson, L. K. and Trosko, J. E. (2005). Oct4 expression in adult human stem cells: evidence in support of the stem cell theory of carcinogenesis. *Carcinogenesis* **26**, 495-502.
Takada, T., Iida, K., Awaji, T., Itoh, K., Takahashi, R., Shibui, A., Yoshida, K., Sugano, S. and Tsujimoto, G. (1997). Selective production of transgenic mice using green fluorescent protein as a marker. *Nat. Biotechnol*. **15**, 458-461.
Tarkowski, A. K., Witkowska, A. and Nowicka, J. (1970). Experimental parthenogenesis in the mouse. *Nature* **226**, 162-165.
Volinia, S., Calin, G. A., Liu, C. G., Ambs, S., Cimmino, A., Petrocca, F., Visone, R., Iorio, M., Roldo, C., Ferracin, M. et al. (2006). A microRNA expression signature of human solid tumors defines cancer gene targets. *Proc. Natl. Acad. Sci. USA* **103**, 2257-2261.
Wang, T., Pentyala, S., Elliott, J. T., Dowal, L., Gupta, E., Rebecchi, M. J. and Scarlata, S. (1999). Selective interaction of the C2 domains of phospholipase C-β1 and -β2 with activated Gαq subunits: an alternative function for C2-signaling modules. *Proc. Natl. Acad. Sci. USA* **96**, 7843-7846.
Whittingham, D. G. and Siracusa, G. (1978). The involvement of calcium in the activation of mammalian oocytes. *Exp. Cell Res*. **113**, 311-317.
World Health Organization (2003). *Tumours of the Breast and Female Genital Organs* (ed F. A. Tavassoli and P. Devilee) Lyon: IARCPress-WHO.
Wu, A. T., Sutovsky, P., Manandhar, G., Xu, W., Katayama, M., Day, B. N., Park, K. W., Yi, Y. J., Xi, Y. W., Prather, R. S. et al. (2007). PAWP, a sperm-specific WW domain-binding protein, promotes meiotic resumption and pronuclear development during fertilization. *J. Biol. Chem*. **282**, 12164-12175.
Yoshida, N. and Perry, A. C. F. (2007). Piezo-actuated mouse intracytoplasmic sperm injection (ICSI). *Nat. Protoc*. **2**, 296-304.

Table S1. Expression of different *pPlcz1* promoter constructs in tissues of transgenic mice of different ages

			tg mRNA expression									
			Brain			Testis			l	k	lu	sl
Construct (tg)	Founder	Generation	2 w	4 w	⩾6 w	2 w	4 w	⩾6 w	⩾6 w			
pPlcz→Plcz-FLAG	#49	F3	+/–	+/–	+/–	+/–	++	++	–	–	–	–
	#28	F3	++	++	nd	++	++	nd	+	+	+	+
pPlcz→Plcz-FLAG-IRES-Venus	#38	F4	+/–	nd	–	+	nd	++	–	–	–	–
pPlcz→Cre	PC67	F3	++	+	nd	++	++	nd	+	+	–	–
	PC69	F4	+	–	+	+/–	++	++	–	–	–	–

tg, transgene; w, weeks; l, liver; k, kidney; lu, lung; sl, spleen; nd, no data.
Expression levels, determined by RT-PCR, range from undetected (–), to weak (+/–), to readily detected (+), to strong (++).

-3.5
0.0
3.5
CS832
CS823R
CS823L
CS686R
CS686L
CV833
CV608
CS785
CS809
wt-ov
wt-plac
CV885
CS110
CS513